



Recovery of High-Added Value Materials from Vinasse Using Laser-Based Combustion

Hassan Nabeel Hassan Mustafa¹, Ahmed Mansor Taha Alzain², Mohammed U. Orsod³,
Ali A. S. Marouf^{3*}

¹Department of Physics, College of Science, Sudan University of Science and Technology, Khartoum, Sudan

²Methanol Chemicals Company, Aljubail, KSA

³Department of Laser Engineering and Industrial Applications, Institute of Laser, Sudan University of Science and Technology, Khartoum, Sudan

Email: hassanhnh2@gmail.com, mr.ahmed01992@gmail.com, mohursod@gmail.com, *marouf.44@gmail.com

How to cite this paper: Mustafa, H.N.H., Alzain, A.M.T., Orsod, M.U. and Marouf, A.A.S. (2023) Recovery of High-Added Value Materials from Vinasse Using Laser-Based Combustion. *Open Access Library Journal*, 10: e9672.

<https://doi.org/10.4236/oalib.1109672>

Received: December 10, 2022

Accepted: February 19, 2023

Published: February 22, 2023

Copyright © 2023 by author(s) and Open Access Library Inc.

This work is licensed under the Creative Commons Attribution International License (CC BY 4.0).

<http://creativecommons.org/licenses/by/4.0/>



Open Access

Abstract

Vinasse is a liquid produced during the process of fermentation and distillation of molasses for the production of ethanol. This paper studies the conversion of vinasse into valuable materials using laser, and the characterization of the provided products. For this purpose, vinasse sample was dried and combusted for 30 seconds using Nd: YAG laser with wavelength 1064 nm at output power 60 W continuous mode. The product of this process was characterized by an X-ray diffractometer (XRD), Fourier transform infrared (FTIR) and X-ray fluorescence (XRF) in order to investigate its crystal structure, functional groups and chemical elements, respectively. XRD results of the combusted vinasse showed Iron Silicide and Sodium Carbonate-Beta in different phases. FTIR showed several absorbance peaks confirming the presence of Iron Silicide and Sodium Carbonate. Moreover, percentages of 0.27% of iron, 0.06% of chrome and 0.01% of nickel were found using XRF.

Subject Areas

Environmental Chemistry, Material Experiment

Keywords

Agricultural Waste Ash, Laser-Based Combustion, Laser-Matter Interaction, Sugarcane Residues, Waste Utilization

1. Introduction

One of the most important residues in the sugarcane farms that are produced

from the extraction of ethanol is Vinasse, which is a liquid produced by the process of fermentation of molasses for the production of alcohol and various yeasts. It has turned the attention of scientists to try to benefit from this article in many different areas for the sake of cleanliness environment. Vinasse is produced in large quantities based on the quality of molasses ranging from 12 to 20 litres versus 1 litre of pure alcohol. Vinasse is used after anaerobic digestion by bacteria and then burned in large kilns to produce potassium-rich fertilizer and used for soil fertilization (Naspolini *et al.*, 2017) [1].

Many researchers have studied the utilization of agricultural wastes and agriculture by-products to obtain useful and valuable materials, including the synthesizing, preparation and extraction of nanostructured materials, such as silica, silica gel, soluble sodium silicate or other materials by different extraction methods (Ma *et al.*, 2012 [2]; Rungrodnimitchai *et al.*, 2017 [3]; Owoeye and Isinkaye, 2017 [4]). Some methods were environmentally friendly techniques (Ghorbani *et al.*, 2015) [5]. There is a growing interest in the extraction of silica nanoparticles and valuable materials from agriculture by-products and waste such as from wheat bran and sesame seed cake (Gawbah *et al.*, 2017 [6]; Gawbah *et al.*, 2018 [7]). A variety of methods has been adopted in literature for this purpose, for example, the extraction of the biogenic silica from samples of some alpine plant species (Carnelli *et al.*, 2001) [8]. Awad *et al.* develop a new procedure for the production of silica powder from sorghum bran ash via laser-based combustion (Awad *et al.*, 2020) [9]. Some researchers study the use of vinasse as a culture medium for bio-surfactant production (Naspolini *et al.*, 2017) [1], or obtain biogas from vinasse bio-digestion (Salomon *et al.*, 201) [10].

Vinasse is considered an extractable substance and a soil-damaging substance where the soil will lose its fertility after five years. Therefore, this work tries to convert it into useful material through combustion by laser. The purpose of this research is to develop a combustion method, for agricultural waste has both positive environmental and economic impacts in utilizing agricultural wastes and agriculture by-products to obtain useful and valuable materials, and it will decrease the cost of waste disposal at the same time.

2. Materials and Methods

2.1. Materials

The sample of liquid vinasse was obtained from Kinana Sugar Plantation Company, Sudan. It was dried under the sunlight for two days without contamination.

2.2. Methods

The Vinasse sample was placed into a high-temperature glass beaker (Schott Duran—Germany) and it was combusted on the air by the heat generated from Nd: YAG laser (Dornier Medilasfibertom to 5100) with wavelength 1064 nm, continuous mode at output power 60 W for 30 s. The laser beam was delivered

by single-mode fibre optic with a diameter of 125 μm . The distance between the sample and the end of the fiber optic was about 1 cm. Because of the small spot size of the laser beam, the process of burning was done point per point. The laser was fixed on a holder while the high-temperature glass beaker was rotated every 30 s carefully for approximately 5 mm. The resulting material was ground carefully with agate mortar for homogeneity. The red laser spot also serves as a target, indicating where the sampling laser will be focused.

2.3. Characterization and Analysis

The X-ray diffraction (XRD) characterization was performed with XRD diffractometer (Shimadzu, MAX_X, XRD-7000) using $\text{Cu K}\alpha$ with scanning speed of $1000^\circ/\text{mi}$, it was used to examine the structure of the sample after combustion process. XRF Analysis was carried out using oxford instruments X-MET5000 Handheld XRF Analyzer. Fourier transform infrared (FTIR) spectrometer (Satellite FTIR 5000) was used for the determination of the functional groups present in the combusted vinasse. FTIR spectrum was collected in the range of $(400 - 4000) \text{ cm}^{-1}$.

3. Results and Discussions

3.1. XRD Analyzing

Figure 1 shows the XRD pattern of the combusted vinasse. The analysis of XRD pattern revealed the presence of two subjects, they were iron silicide (1/1) with a concentration of 94.2% and sodium carbonate-beta with a concentration of 5.8%. **Table 1** and **Table 2** show the miller coordinates in the two subjects.

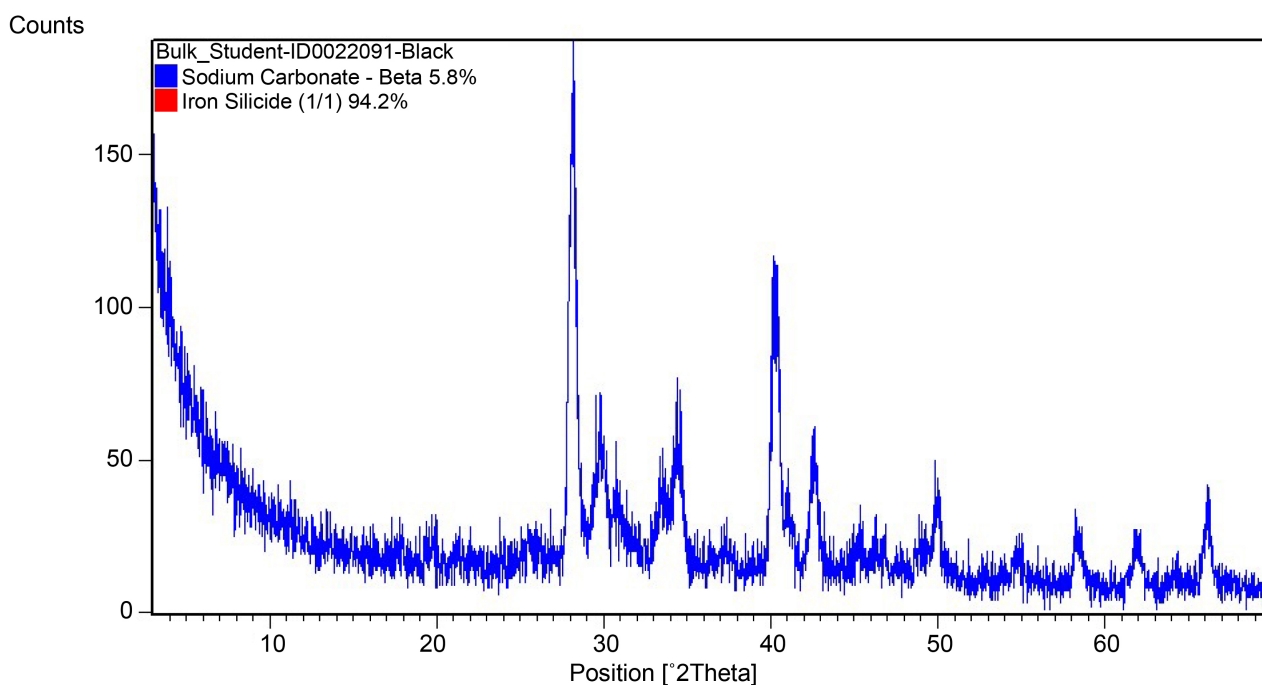


Figure 1. Combusted vinasse XRD pattern.

Table 1. Miller coordinates of sodium carbonate-beta were found in the subject.

H	k	L	Assignment
0	0	1	Sodium Carbonate – Beta
2	0	0	Sodium Carbonate – Beta
1	1	0	Sodium Carbonate – Beta
2	0	-1	Sodium Carbonate – Beta
1	1	-1	Sodium Carbonate – Beta
2	0	1	Sodium Carbonate – Beta
1	1	1	Sodium Carbonate – Beta
0	0	2	Sodium Carbonate – Beta
2	0	-2	Sodium Carbonate – Beta
3	1	0	Sodium Carbonate – Beta
1	1	-2	Sodium Carbonate – Beta
0	2	0	Sodium Carbonate – Beta
1	1	2	Sodium Carbonate – Beta
2	0	2	Sodium Carbonate – Beta
3	1	-1	Sodium Carbonate – Beta
3	1	1	Sodium Carbonate – Beta
0	2	-1	Sodium Carbonate – Beta
0	2	1	Sodium Carbonate – Beta
4	0	0	Sodium Carbonate – Beta
2	2	0	Sodium Carbonate – Beta
4	0	-1	Sodium Carbonate – Beta
2	2	-1	Sodium Carbonate – Beta
4	0	1	Sodium Carbonate – Beta
2	2	1	Sodium Carbonate – Beta
0	0	3	Sodium Carbonate – Beta
3	1	-2	Sodium Carbonate – Beta
0	2	2	Sodium Carbonate – Beta
0	2	-2	Sodium Carbonate – Beta
3	1	2	Sodium Carbonate – Beta
2	0	-3	Sodium Carbonate – Beta
1	1	-3	Sodium Carbonate – Beta
1	1	3	Sodium Carbonate – Beta
2	0	3	Sodium Carbonate – Beta
4	0	-2	Sodium Carbonate – Beta
2	2	-2	Sodium Carbonate – Beta
4	0	2	Sodium Carbonate – Beta
2	2	2	Sodium Carbonate – Beta
4	0	2	Sodium Carbonate – Beta
2	2	2	Sodium Carbonate – Beta
5	1	0	Sodium Carbonate – Beta
4	2	0	Sodium Carbonate – Beta

Continued

1	3	0	Sodium Carbonate – Beta
5	1	-1	Sodium Carbonate – Beta
3	1	-3	Sodium Carbonate – Beta
4	2	-1	Sodium Carbonate – Beta
5	1	1	Sodium Carbonate – Beta
4	2	1	Sodium Carbonate – Beta
1	3	-1	Sodium Carbonate – Beta
0	2	-3	Sodium Carbonate – Beta
0	2	3	Sodium Carbonate – Beta
1	3	1	Sodium Carbonate – Beta
3	1	3	Sodium Carbonate – Beta
0	0	4	Sodium Carbonate – Beta
4	0	-3	Sodium Carbonate – Beta
2	2	-3	Sodium Carbonate – Beta
2	2	3	Sodium Carbonate – Beta
4	0	3	Sodium Carbonate – Beta
2	2	3	Sodium Carbonate – Beta
5	1	-2	Sodium Carbonate – Beta
4	2	-2	Sodium Carbonate – Beta
6	0	0	Sodium Carbonate – Beta
2	0	-4	Sodium Carbonate – Beta
3	3	0	Sodium Carbonate – Beta
1	3	-2	Sodium Carbonate – Beta
1	1	-4	Sodium Carbonate – Beta
5	1	2	Sodium Carbonate – Beta
1	3	2	Sodium Carbonate – Beta
4	2	2	Sodium Carbonate – Beta
1	1	4	Sodium Carbonate – Beta
2	0	4	Sodium Carbonate – Beta
6	0	-1	Sodium Carbonate – Beta
6	0	1	Sodium Carbonate – Beta
3	3	-1	Sodium Carbonate – Beta
3	3	1	Sodium Carbonate – Beta
6	0	-2	Sodium Carbonate – Beta
3	1	-4	Sodium Carbonate – Beta
3	3	-2	Sodium Carbonate – Beta
6	0	2	Sodium Carbonate – Beta
0	2	-4	Sodium Carbonate – Beta
0	2	4	Sodium Carbonate – Beta
3	3	2	Sodium Carbonate – Beta
4	2	-3	Sodium Carbonate – Beta
3	1	4	Sodium Carbonate – Beta

Table 2. Miller coordinates of iron silicide were found on the subject.

h	K	L	Assignment
0	1	1	Iron Silicide (1/1)
1	1	1	Iron Silicide (1/1)
0	1	2	Iron Silicide (1/1)
0	2	1	Iron Silicide (1/1)
1	1	2	Iron Silicide (1/1)
0	2	2	Iron Silicide (1/1)
0	1	3	Iron Silicide (1/1)
0	3	1	Iron Silicide (1/1)
1	2	2	Iron Silicide (1/1)

Table 3. Results of FT-IR analyze.

FTIR shift	Functional	Reference
617.83	C-H stretching	(Makawa, 2016) [11]
670		
869.64	FeFeOH	(Goodman <i>et al.</i> , 1976) [12]
1114.74	SiO-Si stretching band	(Moenke, 1974) [13]
1400.71	Na ₂ CO ₃	(Reig, <i>et al.</i> , 2002) [14]
1622.25	stretching vibrations of -C=N	(Zheng, 2015) [15]

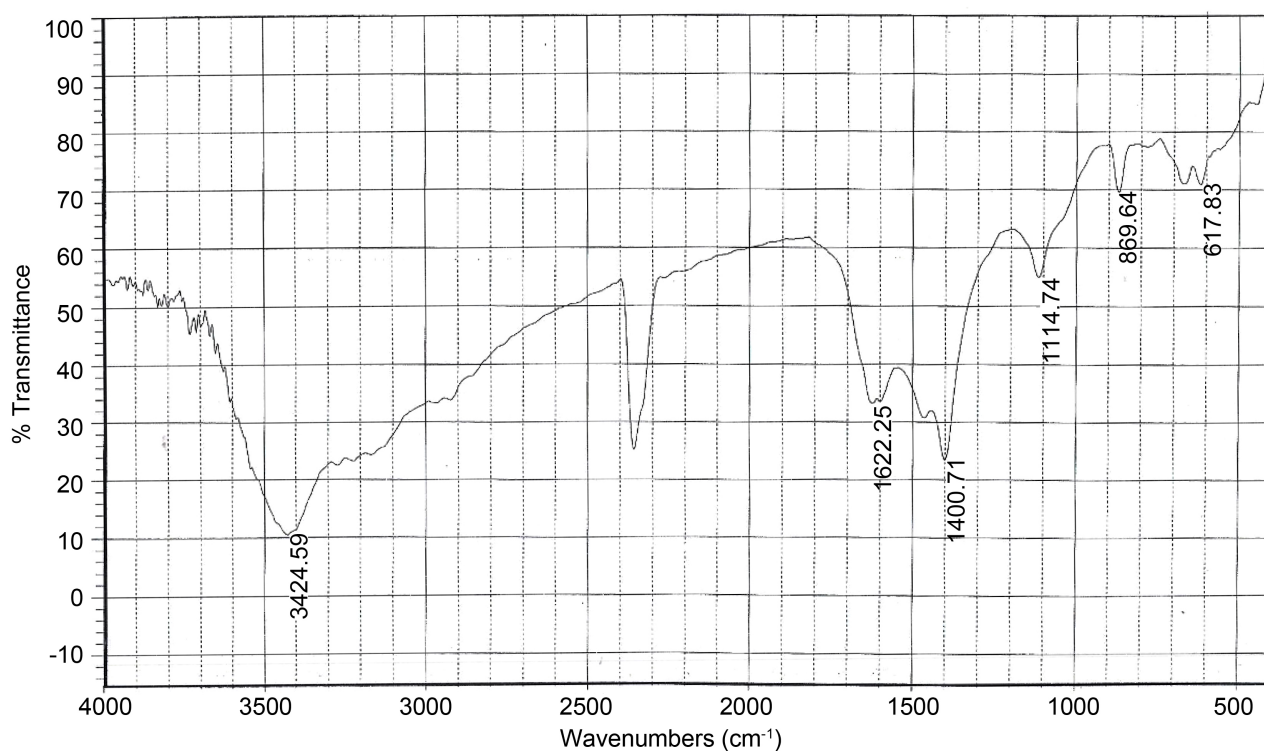
**Figure 2.** FT-IR spectrum of combusted vinasse.

Table 4. XRF analysis after burning.

Analyze Element	Concentration	STD
Cr	0.06%	0.020
Mn	0.00%	0.008
Fe	0.27%	0.028
Ni	0.01%	0.002
Cu	0.00%	0.003
Zn	0.00%	0.002
Pb	0.00%	0.003

3.2. TIR Result

The IR Spectrum was carried out to get information about the entire molecular structure (functional groups) of the combusted vinasse sample. The spectral bands that exist in the FTIR spectrum of the sample are depicted in **Figure 2**. As shown in **Table 3**, the absorbance peak around 617.83 cm^{-1} is attributed to C-H stretching (Makawa, 2016) [11], beak at 869.64 cm^{-1} FeFeOH (Goodman *et al.*, 1976) [12], beak at 1114.74 cm^{-1} SiO-Si stretching (Moenke, 1974) [13], beak at 1400.71 cm^{-1} Na_2CO_3 (Reig *et al.*, 2002) [14] and beak at 1622.25 cm^{-1} stretching vibrations of $-\text{C}=\text{N}$ (Zheng, 2015) [15].

3.3. XRF Analyze

XRF analysis reveals some elements like Chrome by a ratio of 0.06%, Iron by a ratio of 0.27% and Nickel by a ratio of 0.01%. Some elements like Manganese, Zinc, Copper and Lead weren't found (**Table 4**).

4. Conclusions

In conclusion, the obtained Vinasse sample was combusted using Nd: YAG laser continuous mode at output power 60 W for 30 s. The produced materials were ground and then characterized. Based on the results of the XRF device analysis, there was a percentage of iron metal. The results of these tests were confirmed by the results of the XRD examination, which indicates that there is a ratio of 94.2 of iron silicide and Sodium carbonate by 5.8% and confirmed by FTIR analysis because Iron, Silicone and Sodium Carbonate function was found. This result approves this subject formed by Sodium Carbonate and Iron Silicide.

Conflicts of Interest

The authors declare no conflicts of interest.

References

- [1] Napolini, B.F., Machado, A.C.D.O., Cravo Junior, W.B., Freire, D.M.G. and Cammarota, M.C. (2017) Bioconversion of Sugarcane Vinasse into High-Added Value Products and Energy. *BioMed Research International*, **2017**, Article ID: 8986165.

- <https://doi.org/10.1155/2017/8986165>
- [2] Ma, X., Zhou, B., Gao, W., Qu, Y., Wang, L., Wang, Z. and Zhu, Y. (2012) A Recyclable Method for Production of Pure Silica from Rice Hull Ash. *Powder Technology*, **217**, 497-501. <https://doi.org/10.1016/j.powtec.2011.11.009>
- [3] Rungrodnimitchai, S., Phokhanusai, W. and Sungkhaho, N. (2017) Preparation of Silica Gel from Rice Husk Ash Using Microwave Heating. *Journal of Metals, Materials and Minerals*, **19**, 45-50.
- [4] Owoeye, S.S. and Isinkaye, O.E. (2017) Effects of Extraction Temperature and Time on the Physical Properties of Soluble Sodium Silicate from Rice Husk Ash. *Science Journal of Chemistry*, **5**, 8. <https://doi.org/10.11648/j.sjc.20170501.12>
- [5] Ghorbani, F., Sanati, A.M. and Maleki, M. (2015) Production of Silica Nanoparticles from Rice Husk as Agricultural Waste by Environmental Friendly Technique. *Environmental Studies of Persian Gulf*, **2**, 56-65.
- [6] Gawbah, M.A.P., Marouf, A.A., Alsabah, Y.A., Orsod, M.U. and Elbadawi, A.A. (2017) Synthesis of Silica, Silicon Carbide and Carbon from Wheat Bran and Converting Its Crystal Structure Using Nd:YAG Laser. *Future*, **2**, 9.
- [7] Gawbah, M.A.P., Elbadawi, A.A., Alsabah, Y.A., Orsod, M.U. and Marouf, A.A. (2018) Characterization of the Crystal Structure of Sesame Seed Cake Burned by Nd: YAG Laser. *Journal of Materials Science and Chemical Engineering*, **6**, 121. <https://doi.org/10.4236/msce.2018.64013>
- [8] Carnelli, A.L., Madella, M. and Theurillat, J.P. (2001) Biogenic Silica Production in Selected Alpine Plant Species and Plant Communities. *Annals of Botany*, **87**, 425-434. <https://doi.org/10.1006/anbo.2000.1355>
- [9] Awad, A.A.G., Gawbah, M.A.P., Orsod, M.U., Alsabah, Y.A. and Marouf, A.A. (2020) Investigation of the Effects of Laser-Based Combustion on Sorghum Bran. *Albaydha University Journal*, **2**, 52-59. <https://doi.org/10.56807/buj.v2i2.52>
- [10] Salomon, K.R., Lora, E.E.S., Rocha, M.H. and Almazán, O.O. (2011) Cost Calculations for Biogas from Vinasse Biodigestion and Its Energy Utilization. *Sugar Industry*, **136**, 217-223. <https://doi.org/10.36961/si11311>
- [11] Makawa, T. (2016) Adsorptive Potential of Maize Tassel-Ethyl Acrylate Biopolymer Embedded Magnetic Nanohybrid towards the Removal of Cd(II) from Aqueous Solution: An Experimental Design Methodology.
- [12] Goodman, B.A., Russell, J.D., Fraser, A.R. and Woodhams, F.W.D. (1976) A Mössbauer and IR Spectroscopic Study of the Structure of Nontronite. *Clays and Clay Minerals*, **24**, 53-59. <https://doi.org/10.1346/CCMN.1976.0240201>
- [13] Moenke, H.H.W. (1974) Silica, the Three-Dimensional Silicates, Borosilicates and Beryllium Silicates. In: Farmer, V.C., Ed., *Infrared Spectra of Minerals*, Mineralogical Society Monograph 4, Adlard & Son, Surrey, 365.
- [14] Reig, F.B., Adelantado, J.G. and Moreno, M.M. (2002) FTIR Quantitative Analysis of Calcium Carbonate (Calcite) and Silica (Quartz) Mixtures Using the Constant Ratio Method. Application to Geological Samples. *Talanta*, **58**, 811-821. [https://doi.org/10.1016/S0039-9140\(02\)00372-7](https://doi.org/10.1016/S0039-9140(02)00372-7)
- [15] Zheng, J. and Ma, L. (2015) Silver (I) Complexes of 2, 4-dihydroxybenzaldehyde-amino Acid Schiff Bases—Novel Noncompetitive α -Glucosidase Inhibitors. *Bioorganic & Medicinal Chemistry Letters*, **25**, 2156-2161. <https://doi.org/10.1016/j.bmcl.2015.03.078>